Seventeenth Quarterly Progress Report

August 1, 2010 to October 31, 2010
Contract No. HHS-N-260-2006-00005-C
Neurophysiological Studies of Electrical Stimulation for the Vestibular Nerve

Submitted by:
James O. Phillips, Ph.D.[1,3,4]
Steven Bierer, Ph.D. [1,3,4]
Albert F. Fuchs, Ph.D. [2,3,4]
Chris R.S. Kaneko, Ph.D. [2,3]
Leo Ling, Ph.D. [2,3]
Shawn Newlands, M.D., Ph.D. [5]
Kaibao Nie, Ph.D. [1,4]
Jay T. Rubinstein, M.D., Ph.D. [1,4,6]

[1] Department of Otolaryngology-HNS, University of Washington, Seattle, Washington
[2] Department of Physiology and Biophysics, University of Washington, Seattle, Washington
[3] Washington National Primate Research Center, University of Washington, Seattle, Washington
[4] Virginia Merrill Bloedel Hearing Research Center, University of Washington, Seattle, Washington
[5]Department of Otolaryngology, University of Rochester, Rochester, New York
[6] Department of Bioengineering, University of Washington, Seattle, Washington

Reporting Period: August 1, 2010 to October 31, 2010

Challenges: Our real time frequency modulated stimulation strategy still has a significant response lag between the head velocity input and eye velocity output. In Quarter 16, we created software running on the Cochlear SDK platform that was capable of taking an analog input signal and generating frequency-modulated (FM) pulse trains in real-time. Our animal experiments and bench top tests suggested that the software was able to perform the correct transformation, however the response latency was too long (a variable latency 30-60 ms) and was also dependent on the pulse modulation rate. We observed and reported a variable latency of 30-60 ms in response to steps of velocity input. In Quarter 17, significant effort was devoted to changing the pulse train streaming structure to minimize the FM transformation latency. With the new design, the minimal latency we are able to achieve has been reduced to 10 ms. The response latency is consistent and not variable, but it is still longer than we would like.

Our response to the original challenge was to change to entire pulse setting paradigm. In the previous implementation, the software set the period of each single pulse according to the pulse rate calculated from the analog input signal. For example, the pulse period is set to 20 ms if the corresponding pulse rate is 50 pps. The pulse-setting paradigm can cause a long latency because it takes 3 or more pulse periods to respond to a change in the analog input signal. The pulse buffer in the stimulus controller of the cochlear SDK platform contributed a variable delay. In the current design, we use a completely different strategy to generate pulses. A pulse train with a longer period is implemented with several shorter pulses at a period of 1 ms. For example, the period of a 50 pps pulse is divided into 20 pulses with a period of 1 ms each. Most of the pulses are given an amplitude of ≈0 μA. This new implementation allows a quick update of the streaming pulse buffer if a change in the analog input signal is detected. We have implemented the new design and we are currently in the process of further code debugging and improvement. To further improve the performance of the real time frequency modulated stimulation, in Quarter 18 we will work with our new software to minimize the delay caused by each source in order to achieve an overall latency less than 10 ms. We will evaluate latency on the bench and in vivo in response to input changes. It is not clear how much further we can reduce the response latency by improving code efficiency. The latency could be a result of multiple sources such as analog-to-digital conversion, transfer of data between digital signal processors, pulse streaming buffer size and signal processing delay. Although we are shifting our emphasis from development to testing in the remaining quarters, we recognize that optimizing our real time capability is critical for the success of our contract aims.

Successes: We have made important progress in several areas as noted below.

1. We have now developed a flexible system for controlling real time amplitude modulated stimulation via the clinical processor. This computer-based interface allows us to manipulate the transformation of head velocity signals into an appropriate input for driving eye velocity through the implant. As will be demonstrated below, this

may be critically important because eye velocity shows significant changes with changes in the frequency of the head velocity stimulus and with changes in eye position. This new controller will allow us to optimize our electrical stimulation parameters empirically during real time stimulation.

In Quarter 17, we improved the signal-delivery interface to the Cochlear Freedom clinical processor, which provides real-time stimulus control of the vestibular implant. Like the analog approach based on the Nuclear-Chicago stimulator (QPR 16), the new interface offers fast triggering of brief pulse trains over a range of voltage-controlled current levels. However, because it is based on the MATLAB programming environment, the new approach is more flexible, allowing continuous modulation of pulse trains based on an external signal (e.g. chair velocity) and non-linear voltage-to-current transformation. Control of more than one stimulus channel is also available with this method.

The stimulus interface was programmed in the MATLAB Simulink environment, using the Signal Processing Blockset, Real-Time Workshop, and Real-Time Windows Target toolboxes. The two modes of the program are shown as block diagrams in Figure 1, for single-channel processing. Both modes acquire and deliver signals with a data acquisition board (National Instruments PCI-MIO-16XE-50). In trigger mode (Figure 1A), a TTL pulse initiates a waveform (band limited to ~100 Hz) that modulates a 1 kHz sinusoidal carrier. The resulting AM signal is conveyed to the output channel of the DAQ board, conditioned with an audio amplifier, and sent to the auxiliary audio jack of the clinical interface. In signal mode (Figure 1B), the modulating input signal is itself acquired and appropriately transformed before mixing with the carrier.

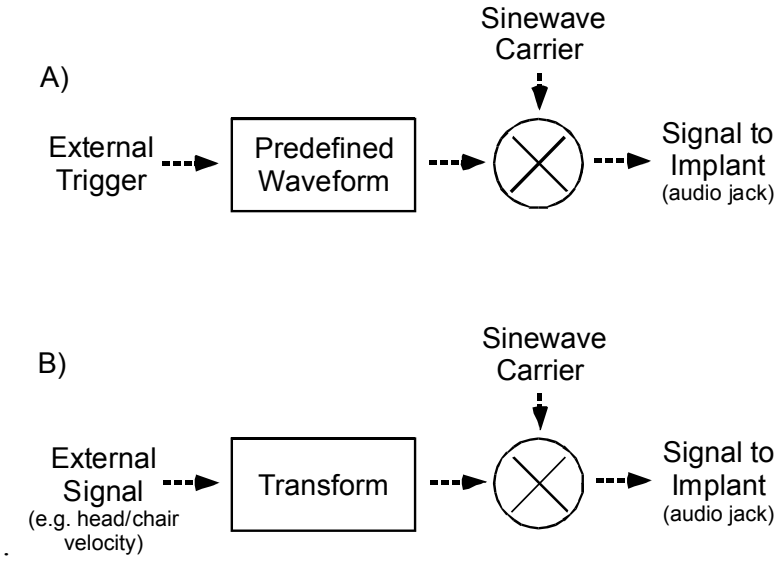

Figure 1. *Block diagrams of the stimulus delivery Simulink program for (A) trigger mode and (B) stimulus mode.*

While only one modulation/stimulation channel is illustrated in Fig. 1, multiple channels can be handled by mixing each modulation signal with a different carrier frequency (e.g. 1 kHz and 4 kHz) and summing the result. The different carriers would subsequently be

parsed by the clinical processor. In this manner, simultaneous real-time stimulation of two or three canals is possible. Because only the envelope of the AM signal is extracted by the implant processor in signal mode (i.e. phase information is lost), the modulating signal should be non-negative and scaled to the audio specifications of the processor. Two examples of transformations are depicted in Figure 2. If the input signal is chair or head velocity, one possibility is to force all negative velocities to zero (Figure 2A). In this case, only positive (excitatory) velocities would be encoded by the implant. Alternatively, negative velocities can be encoded by biasing the modulation signal to a positive voltage when the velocity is zero (Figure 2B). A linear input-output relationship is shown here, but the negative and positive velocity components can instead be assigned different gains, creating a piecewise linear transform. Other nonlinear transformations, such as sigmoidal functions, can also be implemented.

The clinical processor was programmed as in QPR 16 using the Custom Sound 2.0 clinical mapping software. Definable parameters include the channel(s) of stimulation, spectral analysis band(s), pulse width, pulse rate, and current range.

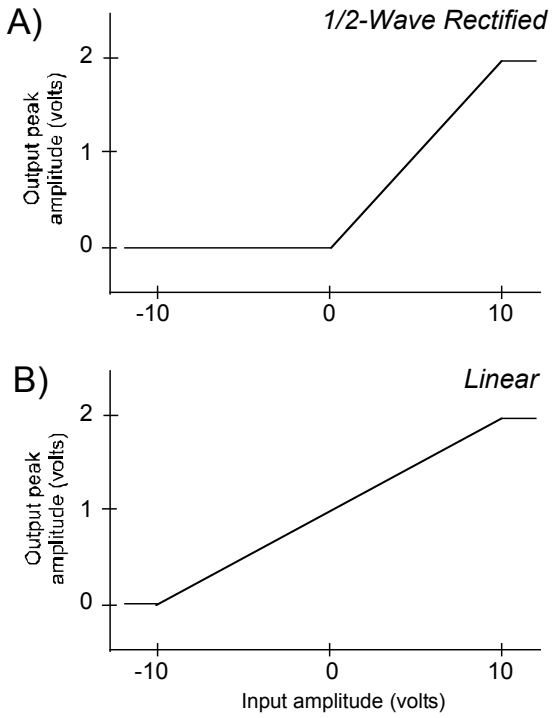

Figure 2. *Non-linear (A) and linear (B) signal mode transformations.*

Testing of the signal delivery program was performed using the "implant-in-a-box", with the output channel connected to ground via a 10 kOhm resistor. An example of the processing of a square wave input signal is shown in Figure 3 at two scales. The external signal (top trace) switches between -10 and +10 volts, representing the range of the chair velocity signal in our lab. The output of the signal delivery program (middle trace) has been nonlinearly transformed using the function in Figure 2A and mixed with a 1 kHz sine wave carrier. The small fluctuations are caused by line noise. The output follows

the original signal with a delay of only ~1 ms, verifying real-time processing. The final electrical pulse train output by the clinical processor (500 pps, 100 μs/phase, threshold = 0 μA, maximum current = 150 μA), closely matches the AM signal with a processing delay of ~14 ms.

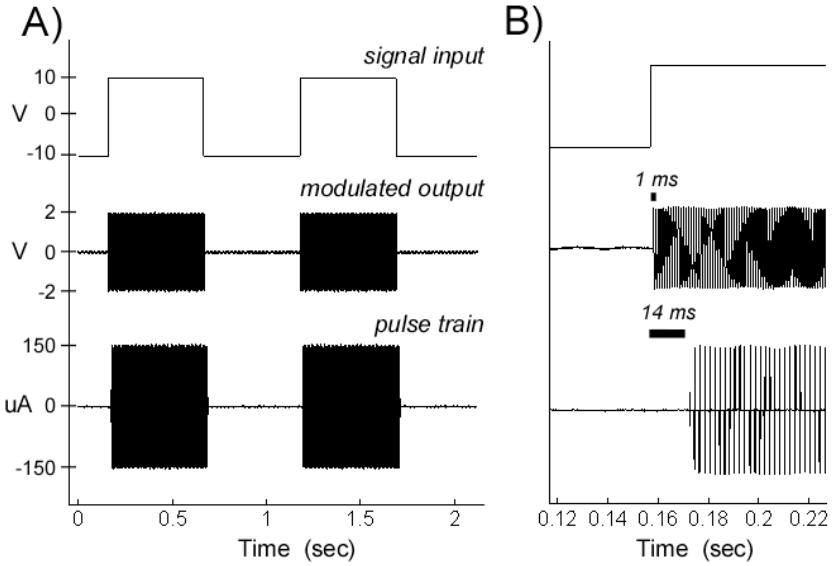

Figure 3. *Example of real-time processing of a square wave input signal. A) Large scale. B) Close-up scale. Horizontal lines indicate the processing delays from the initial upswing of the square wave.*

Two additional examples of real-time processing are shown in Figure 4 for sinusoidal input signals slightly smaller than full range (+/- 9.5 volts). Figure 4A demonstrates nonlinear rectification of the input, so that only the positive portion of the signal is conveyed to the implant processor; note that at the lower current values, the pulse train abruptly drops to zero. This occurs because the minimum current level that the implant processor can produce is ~20 μA. In Figure 4B, with a linear transformation, both the positive and negative phases of the original signal are apparent in the output pulse train.

2. We have now evaluated the changes in eye velocity produced by electrical stimulation of the vestibular end organ at different times during active natural gaze shifts. In order to confirm that vestibular input generated by electrical stimulation is processed as a natural head velocity signal, we stimulated during natural head free gaze shifts. The literature suggests that there is a decrease in the vestibulo-ocular reflex gain during gaze shifts, which facilitates the contribution of head movement to gaze amplitude. Head movement perturbations during gaze shifts produce changes in eye velocity that are lower than those produced during fixation, and differ over the course of a head unrestrained gaze shift. Initially, during the earliest portion of a head free gaze shift, the perturbation has little effect. Then, as the gaze shift progresses, there is an increasing effect of head velocity on eye velocity. We reasoned that if the electrical stimulation was being treated as a head velocity signal, short stimulation trains would produce similar perturbations if summed with an ongoing head unrestrained gaze shift.

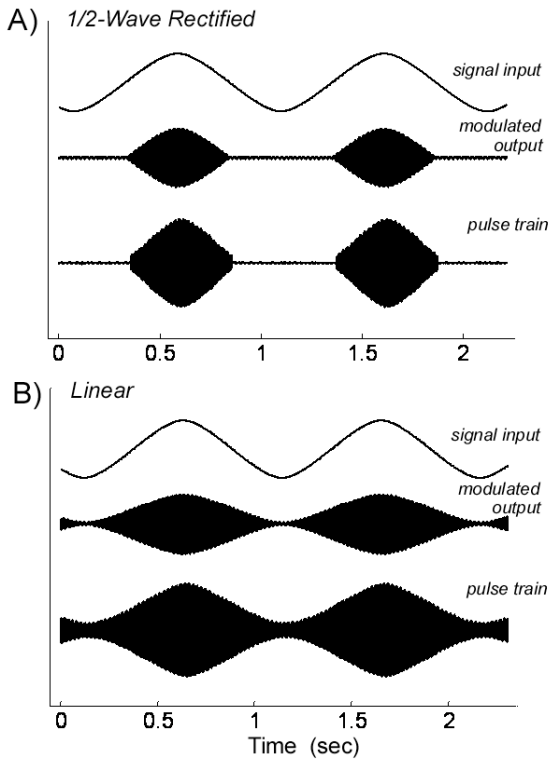

Figure 4. *Two examples of real-time processing of a sine wave input signal. A) Nonlinear, half-wave rectified transform. B) Linear transform. Ordering of traces is the same as Figure 3.*

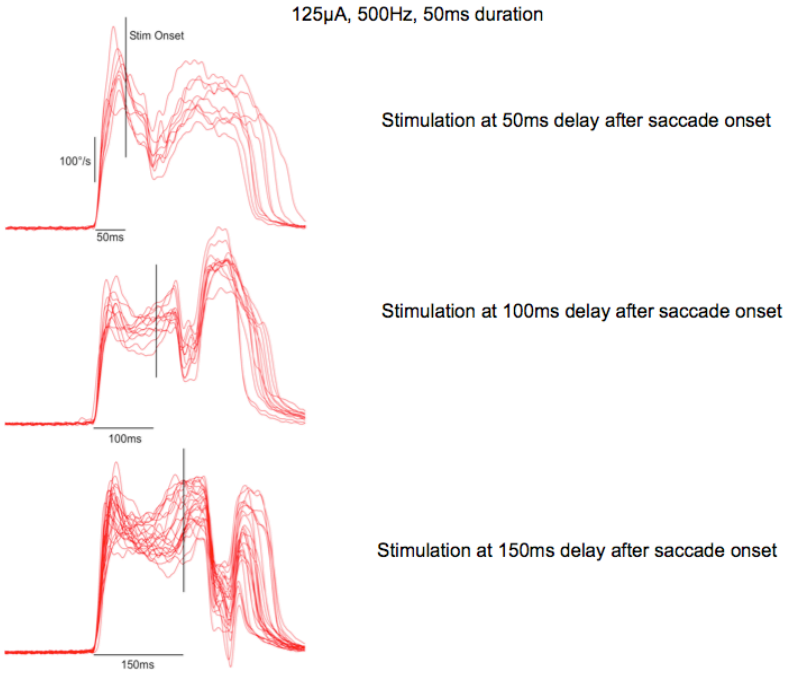

Figure 5. *Gaze velocity during head free gaze shifts with superimposed 50 ms electrical stimulation of the right lateral canal at different times following gaze onset.*

Figure 5 shows the result of one experiment in which we superimposed a 50 ms stimulus train on several gaze shifts at 50, 100 and 150 ms after the onset of the gaze shift. In each set of traces, the vertical bar indicates the stimulation onset command, which leads the onset of electrical stimulation by 14 ms. The resulting velocity profiles show a clear decrease in gaze velocity resulting from electrical stimulation which increases in size as the gaze shift progresses. This result is a demonstration that the electrically elicited velocity input is being processed as a normal head velocity command. Also, because the electrical stimulation is much cleaner than the head perturbation data already in the literature, this is a very nice demonstration of the original phenomenon.

3. We have examined the effect of eye position on the behavior elicited by electrical stimulation of the vestibular nerve. Although we have shown that we can produce reliable eye velocities with electrical stimulation, most of these movements have been initiated from primary orbital position; i.e., straight ahead. Since the vestibular system has direct access to motoneurons, and at different eye positions individual motoneurons will be receiving different levels of tonic input, we reasoned that motoneurons may process the electrically elicited vestibular inputs differently at different eye eccentricities. This may, in turn, produce different eye velocities for the same input. This might be useful in counteracting pathological nystagmus in different eye positions, or it might work against a consistent effect depending on the sign and size of the effect.

To evaluate the difference in eye velocities elicited by electrical stimulation, we presented brief, 50 ms, trains of biphasic pulses to either the lateral or the posterior canal during a tracking task where the monkeys tracked point stimuli to different fixation eccentricities. The target was extinguished at the onset of electrical stimulation. Figure 6 shows that the eye movements that result from such stimulation are strongly influenced by eye position. This is a startling result. As the eye position moved farther to the left, the horizontal eye velocity elicited by right lateral canal stimulation increased, as did the velocity of the oppositely directed eye movement that resulted following stimulation. Also, at different eye positions, the vertical component changed direction. It is clear that a strong eye position effect was present, at least at this stimulus current. It is also clear that these short stimulation trains were not integrated into a tonic eye position command to produce maintained eye position. To check whether this effect was sustained across different stimulation currents producing different eye velocities, we repeated the experiment at different stimulation currents. Figure 6 shows that the results were qualitatively similar for each stimulation current tested. The slope of the relationship between horizontal movement velocity and eye position remained roughly constant, but the velocities increased with increasing current. For vertical velocity, the direction of the eye movement changed at roughly the same horizontal eye position for all currents. In this case, the slope of the relationship increased with increasing current. These two plots suggest a different mechanism for the position effects on the horizontal and vertical component of the stimulation elicited eye movements. Regardless of mechanism, it appears that eye position is an important parameter in the behavioral expression of short duration electrical stimulation. It is critical to understand the mechanism behind this phenomenon because it will potentially influence the efficacy of a vestibular prosthesis.

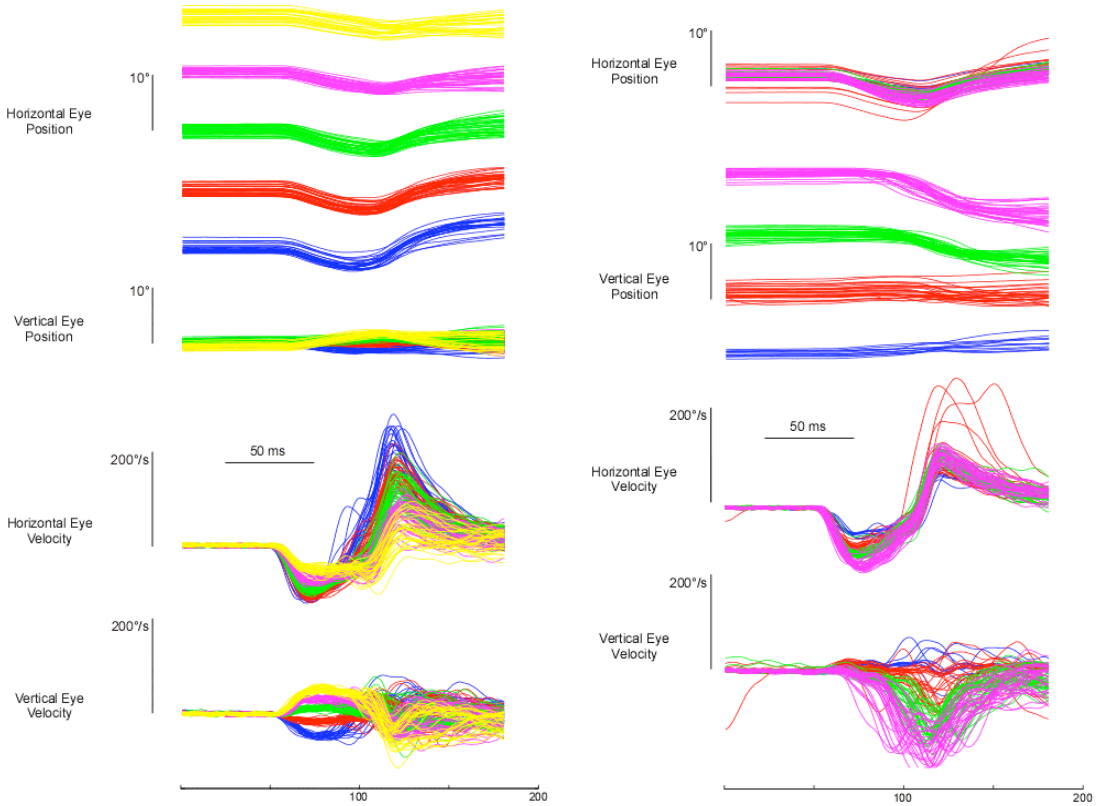

Figure 6. *Eye velocity and position for 50 ms electrical stimulation in the right lateral canal initiated at different eye positions. The colors differentiate the stimulus trials at each eye position. The right column shows trials in which the horizontal position was varied, while the left column shows trials where the vertical eye position was varied.*

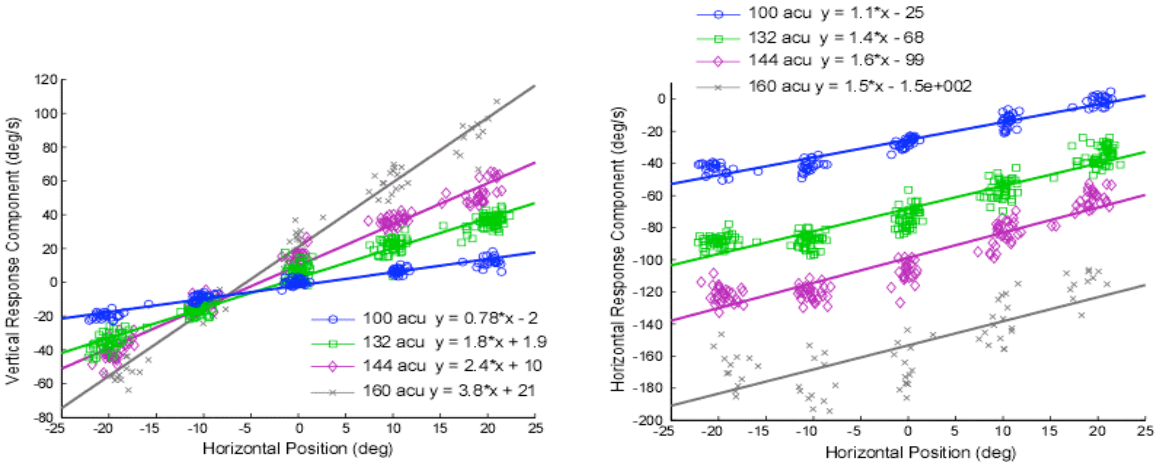

Figure 7. *Vertical and horizontal eye velocity versus horizontal eye position across a number of stimulation currents for electrical stimulation of the right lateral canal.*

4. We have demonstrated that the slow phase eye movement velocity response to electrical stimulation with our device is frequency dependent at higher frequencies. In previous QPRs we have demonstrated that many properties of the eye movement response to electrical stimulation are remarkably nearly linear. However, one aspect of the response that we have not investigated in detail is the frequency response of eye movements during modulated electrical stimulation. Over a range of frequencies from 0.25 to 1.0 Hz, the eye movement response appears to be roughly frequency independent. However, what happens if we push the system to higher frequencies, which are still within the range of the frequencies encountered during normal behavior in monkeys and humans? To answer this question we applied frequency modulated trains of biphasic electrical stimuli to the lateral canal of rhesus monkeys at modulation frequencies from 0.5 to 20 Hz. The eye movements resulting from three representative modulation frequencies are shown in Figure 8.

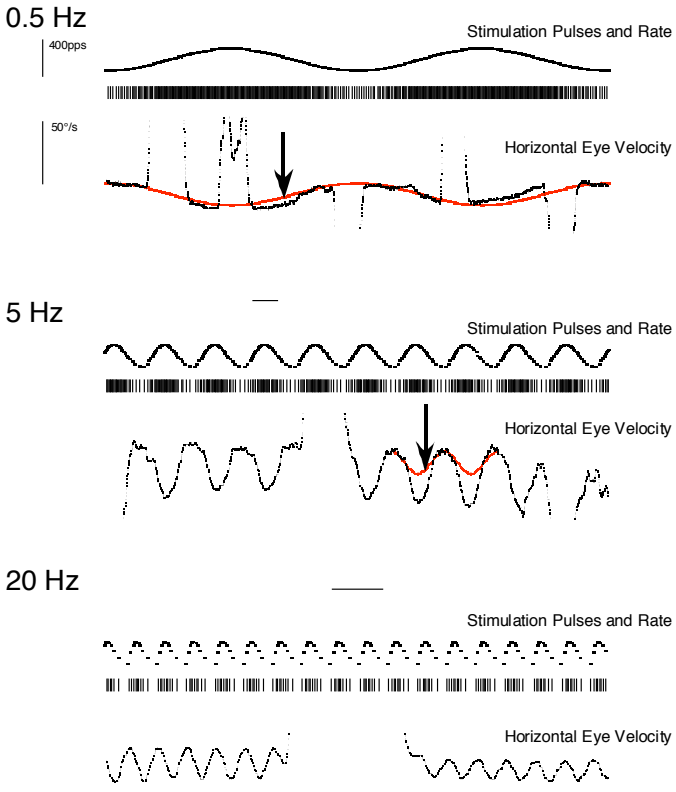

Figure 8: *Eye movements resulting from frequency modulated biphasic pulse trains applied to the right lateral canal (150 µA, 0-400 pps rate, 100 µs per phase, 8 µs interphase gap). The best fit sine wave for the slow phase eye velocity at 0.5 Hz is shown in red (vertical arrow). A similar fit is shown for 5 Hz, but the amplitude of the fit is adjusted to show the predicted eye velocity if the response amplitude was identical to that for the 0.5 Hz fit (vertical arrow).*

Figure 8 demonstrates that there is a change in response peak velocity for higher modulation frequency vestibular stimuli at the same current. For example, the peak velocity of the response at 0.5 Hz is roughly half of that at 5 Hz, while the response at 20

Hz falls somewhere in between. Figure 8 also demonstrates the eye position effect shown in section 3 above. For the 20 Hz data, there is a significant difference between the peak velocities early in the trace (left) and later in the trace (right). This is because there was a large horizontal saccade between these portions of the trace. The change in eye position changed the 20 Hz response amplitude, or peak velocity, without any change in the stimulation parameters.

Figure 9 plots the response amplitude of the best fit sine wave for several frequencies of sine wave frequency modulated stimulation. Each data point represents the eye velocity modulation amplitude for a several cycles of modulated stimulation. The plot shows that there is greater variability in response amplitude to modulation frequencies above 2.0 Hz, and 5 Hz modulation frequencies produce the highest overall response amplitudes. This dynamic characteristic of sine wave modulated stimulation may reflect the high velocity slow phase transient at the start of constant frequency electrical stimulation. It suggests that the optimal stimulation parameters must be adjusted with frequency to produce a constant peak velocity modulated eye movement without significant central adaptation.

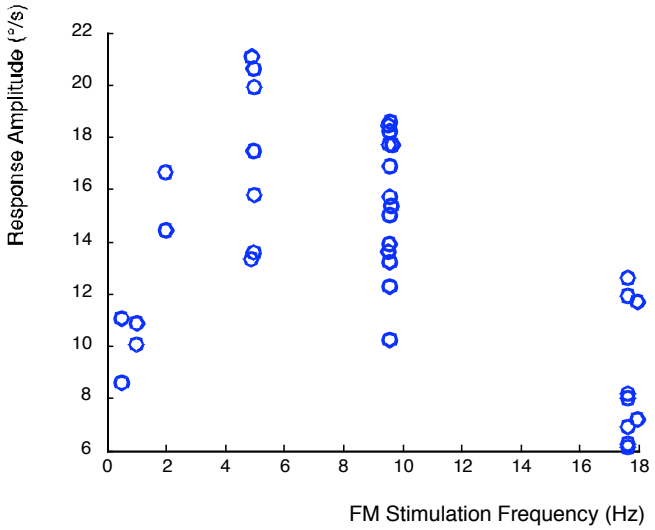

Figure 9. *Response amplitude versus FM modulation frequency. Each point represents the average best fit sine wave amplitude for multiple cycles of sine wave modulated eye velocity at a given modulation frequency during right lateral canal stimulation (150 µA, 0-400 pps rate, 100 µs per phase, 8 µs interphase gap).*

4. We have shown that summation of electrical and rotational stimulation is largely frequency independent between 0.25 and 1.0 Hz. Since there appeared to be a few non-linearities emerging from the analysis of new stimulation paradigms, we decided to revisit the summation of natural rotational and electrical stimulation before doing further recording of neurons during these paradigms. We varied both rotational frequency and stimulation current and observed the offset in slow phase velocity resulting from electrical stimulation at a constant frequency during sinusoidal en-bloc rotation, and the modulation amplitude from the best fit sine wave of eye velocity resulting from the rotation during electrical stimulation. Our results are displayed in Figure 10. Figure 10A shows that with increasing electrical stimulation current there is an increasing offset or DC shift in velocity. The DC shift is very close to the average velocity of the slow phase

of nystagmus elicited during control stimulations (control). Figure 10B shows that although there is a change in modulation amplitude with rotation frequency, there is little change in modulation amplitude with increasing electrical stimulation current. Taken together, these data suggest that there is nearly linear summation of the behavioral eye movement response to combined rotational and electrical stimulation.

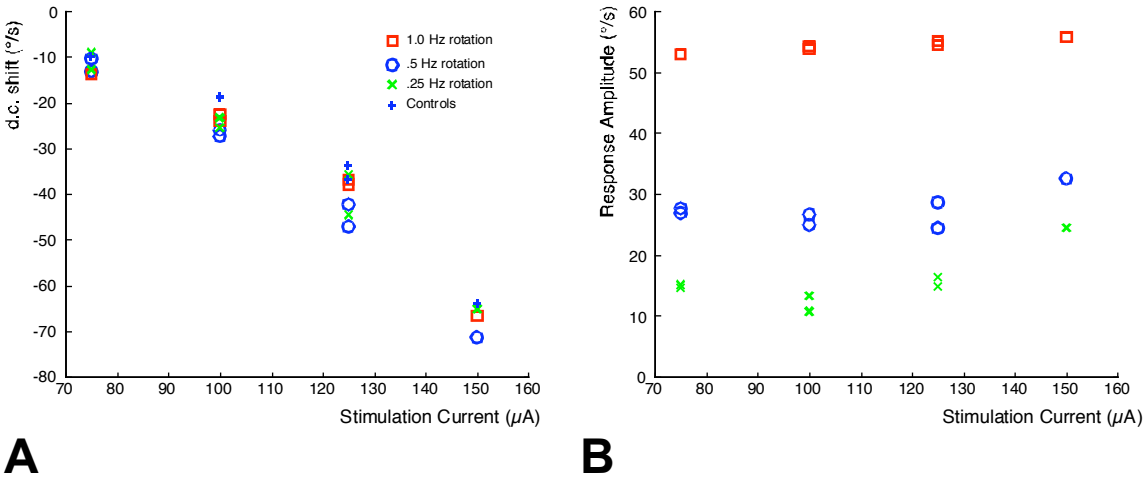

Figure 10. *Offset (DC Shift) and modulation amplitude of slow phase velocity as a function of electrical stimulation current across several frequencies of en bloc rotation during constant rate electrical stimulation. Each data point represents the average of several cycles of rotation at a given stimulation current and rotation frequency.*

5. We have examined the summation of electrically elicited and natural responses in brainstem neurons downstream of the vestibular nucleus. Since we demonstrated that the summation of rotational and electrical stimulation responses occurs behaviorally across a range of frequencies and currents, we decided to further investigate the neuronal mechanism underlying this property. In Quarter 16, we demonstrated that secondary vestibular neurons in the medial vestibular nucleus did not show a summation of electrically elicited and rotationally elicited spike discharge at higher electrical stimulation rates. The response to higher rate stimulation essentially replaced the rotational modulation of such vestibular neurons. It appeared that the summation of the two velocity signals, one rotational and one electrical, was occurring further downstream in the vestibulo-ocular reflex pathway. We reasoned that this summation could be either neural or mechanical, occurring somewhere in the brainstem processing of the velocity signals, or occurring at the level of the oculomotor plant. To distinguish between these two possibilities, we recorded from abducens motoneurons during combined en-bloc rotation about an earth vertical axis and during constant rate electrical stimulation of the lateral semicircular canal, both separately and during combined stimulation. The results of these experiments are shown for a single abducens neuron in Figures 11-14.

Figure 11 displays a frequency histogram and unit raster for the discharge of a typical abducens neuron aligned on the electrical stimulus artifact in response to 10 pps electrical stimulation of the lateral semicircular canal at 125 μA. The first spike following electrical stimulation at 0.0 ms is highlighted in blue for the unit raster. The histogram

below the raster shows that although this neuron discharges at a somewhat longer and more variable latency to the electrical stimulus than a vestibular nucleus neuron, the abducens neuron is driven by the electrical stimulus.

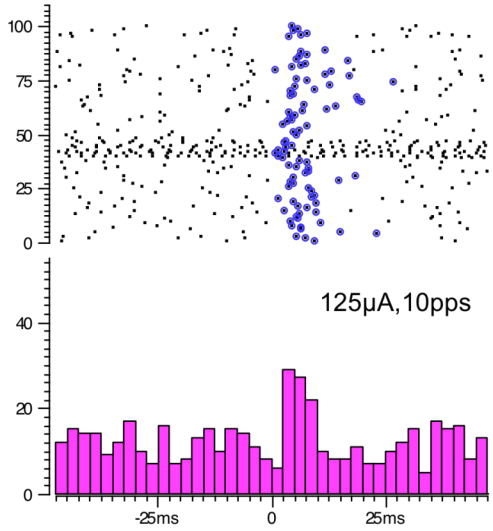

Figure 11. *Typical response of a left abducens neuron to electrical stimulation of the right lateral semicircular canal (monopolar, 10 pps, 125 μA).*

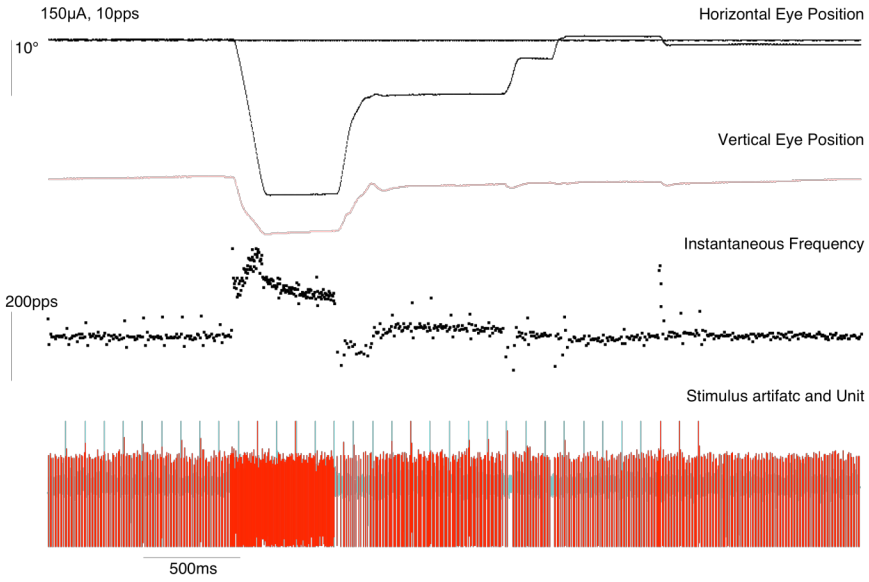

Figure 12. *Instantaneous firing rate of abducens neuron in Figure 11 during 10 pps electrical stimulation. The stimulus artifact is displayed in grey, and the unit discharge is displayed in red. The large red spikes are instances where the unit discharge is superimposed on the stimulus artifact, but was disambiguated by unit identification techniques described in previous QPR reports.*

Figure 12 shows the discharge of the same neuron as in Figure 11 during a fixation task combined with low frequency, 10 pps, electrical stimulation of the contralateral lateral canal. The resulting instantaneous firing rate reflects the presence of intermittent short latency interspike intervals with occasional spikes in the instantaneous firing rate time locked to the electrical stimulus. Also, however, the discharge of the neuron reflects the eye position trace, with a burst and tonic discharge associated with the saccade and fixation to the left. Therefore, at low frequencies of stimulation, the discharge of the abducens neuron reflects both eye position and electrical stimulation.

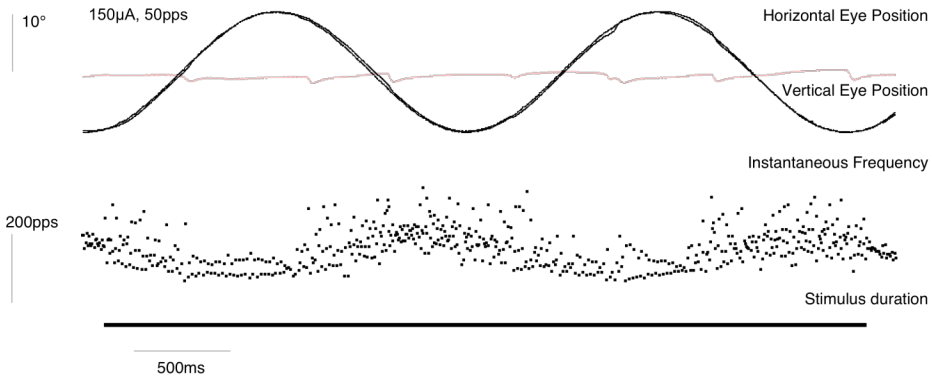

Figure 13. *Instantaneous firing rate of the abducens neuron in Figure 11 during 50 pps electrical stimulation and en-bloc rotation with an earth stationary visual target.*

Figure 13 shows the discharge of the same abducens neuron during electrical stimulation and en-bloc rotation. At this frequency of electrical stimulation there is disruption of the modulation of a typical vestibular nucleus neuron with rotation, but this abducens neuron displays relatively good modulation of discharge with the rotational stimulus. The summation of electrical and rotational inputs is most easily seen in the discharge of the neuron in right gaze (rightward eye positions), where there is an alternating elevation in the instantaneous discharge frequency due to the electrical stimulus.

Figure 14 shows the discharge of the abducens neuron displayed in the preceding figures during en-bloc rotation in the dark combined with 200 pps electrical stimulation of the lateral canal. The discharge of the neuron is still modulated with eye position and, to a lesser extent, eye velocity, as expected for an abducens neuron. The high frequency electrical stimulation adds to the discharge rate of the neuron without eliminating the modulation of the neuron in response to the eye movements elicited by the rotational stimulus. Therefore, this figure demonstrates that at high electrical stimulation rates, which largely eliminate the modulation of electrically driven medial vestibular nucleus neurons, the abducens neuron is performing a summation of electrical and rotational velocity inputs.

Not all abducens neurons show this behavior, however. Figure 15 shows the discharge of a second abducens neuron that was also driven by electrical stimulation. This neuron

responds to changes in eye position with a typical burst tonic pattern of discharge in the absence of electrical stimulation of the lateral canal (not shown).

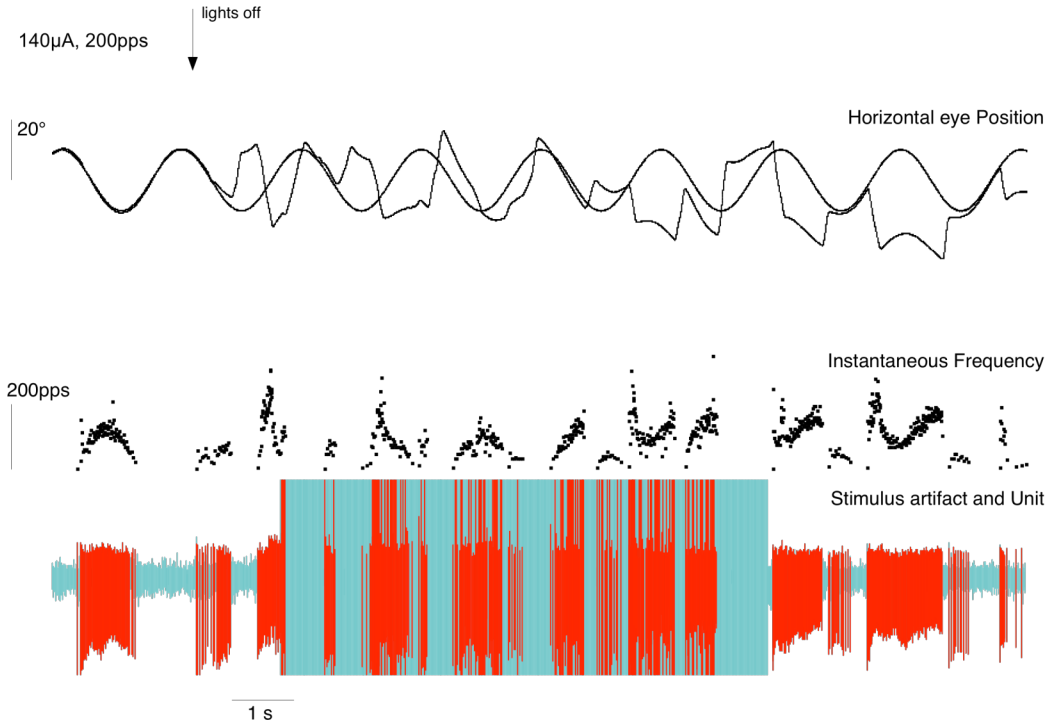

Figure 14. *Discharge of the abducens neuron shown in figure 11 during en-bloc rotation combined with 200 pps electrical stimulation of the lateral canal. The unit discharge is displayed in red and the stimulus artifact is displayed in grey. The large red spikes are instances where the unit discharge is superimposed on the stimulus artifact, but was disambiguated by unit identification techniques described in previous QPR reports.*

In Figure 15, the neuron displayed a short latency discharge in association with electrical stimulation. This can be seen in the overlapping traces of the unit discharge and stimulus artifact shown in the lower right panel of the figure. This time locked discharge is also present during high frequency electrical stimulation, as shown in the unit raster in the lower left hand panel of the figure. In this panel, electrical stimulation at 100 pps produces a time locked discharge in the abducens neuron. In the dark, the electrical stimulation elicits a robust right beating nystagmus as shown in the top panel of Figure 15. The abducens unit would ordinarily be expected to follow eye position in its discharge during nystagmus, pausing for the rightward directed fast phases of the nystagmus and displaying a ramp in discharge associated with the slow phases of the nystagmus. However, this abducens neuron displays only a constant rate discharge associated with the electrical stimulation under these circumstances. This neuron behaves like the medial vestibular nucleus neurons described in QPR 16. It does not show summation of the eye position plus velocity and electrical stimulation inputs, but rather shows a discharge that is dominated by the electrical stimulus alone at higher stimulation rates.

Our preliminary findings suggest that there may be summation of electrical and rotational input both in brainstem neural elements and in the oculomotor plant, downstream of the final motor output in the abducens nucleus. This is supported by the two types of abducens neuron discharge displayed here. However, we do not know whether the abducens neurons that we are recording are motoneurons or internuclear neurons, which project the medial rectus subdivision of the oculomotor nucleus. It remains a possibility that the summation electrical and natural rotational input is entirely neural, and that only internuclear neurons fail to display summation of these inputs in their discharge during combined stimulation.

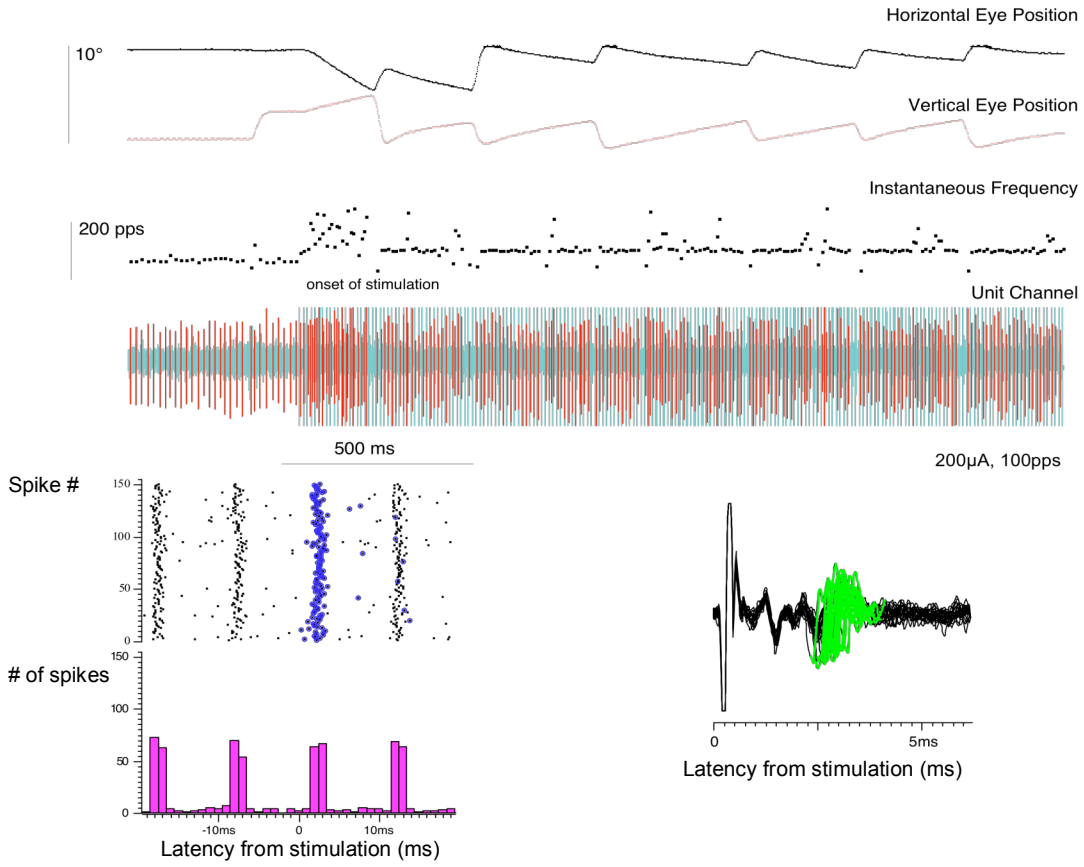

Figure 15: *Discharge of a second abducens neuron, which does not show natural responsiveness during electrical stimulation. Top panel displays the discharge and instantaneous firing rate of the neuron during 100 pps electrical stimulation of the contralateral lateral canal at 200 µA. The unit spikes are in red and the stimulus artifact is in grey. The lower left panel shows a raster of the discharge of the neuron aligned on the occurrence of a stimulus artifact. The first spike following the stimulus artifact is highlighted in blue. The lower right panel shows overlapping traces of neuron discharge in green aligned on the stimulus artifact during 10 pps electrical stimulation.*

6. We have performed first in man implantation of our device and have obtained data consistent with the data obtained in monkeys. Our first human subject was implanted with the device in a four hour surgery using the surgical approach developed in the primates. Because of the relatively larger size and advantageous orientation of the canals in humans, all three canals were implanted successfully. vECAPs were obtained

from the superior and lateral canals at higher thresholds than in the monkeys. A series of intrasurgical vECAP (vestibular evoked compound action potential) recordings were obtained by stimulating a site in one canal and recording from a site in an adjacent canal, as displayed in Figure 16. In Figure 16A, the vECAPs were recorded from electrical stimulation of the superior semicircular canal, while in Figure 16B, the vECAPs were recorded from electrical stimulation of the lateral semicircular canal. In both cases, the size of the recorded potential increases with increasing current, similar to the recordings obtained in the monkeys. Higher currents were required to obtain the cross canal compound action potential recordings in a human subject than for the same canal recordings in the monkeys. The subject did not experience vertigo post surgically and did not have a spontaneous nystagmus in the light. He was discharged from the hospital the next day following the surgery, and returned home.

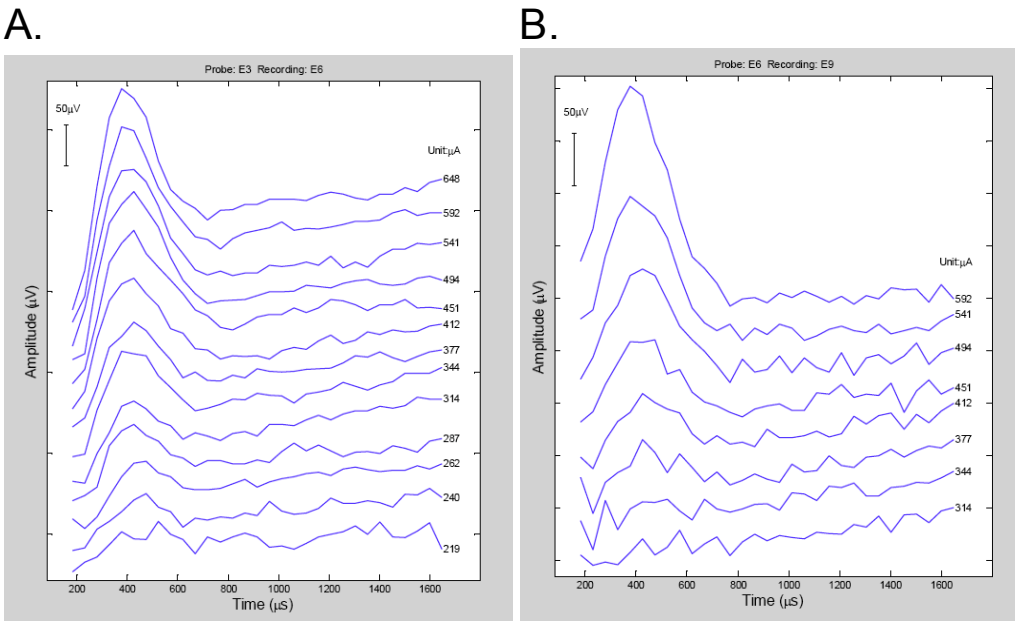

Figure 16. *vECAP recordings from electrical stimulation of the superior (A) and lateral (B) semicircular canals in a human subject.*

7. We have presented our results in scientific meetings during this quarter. The presentation titles and authors are listed below.

Leo Ling, Steven Bierer, Albert F. Fuchs, C. R. S. Kaneko, Kaibao Nie, Shawn Newlands, Amy L. Nowak, Trey Oxford, Jay T. Rubinstein, *James O. Phillips
Towards elucidating the operation of a vestibular prosthesis in the monkey. II: Activation of brainstem neurons and response to high frequency stimulation. NW Auditory and Vestibular Meeting, Seattle, WA, 2010

Amy L. Nowack, Steven Bierer, Albert F. Fuchs, Leo Ling, C. R. S. Kaneko, Kaibao Nie, Shawn Newlands, Trey Oxford, Jay T. Rubinstein, James O. Phillips Effect of eye position on the response of short-duration stimulation trains elicited by electrodes

implanted in the vestibular end organ. NW Auditory and Vestibular Meeting, Seattle, WA, 2010

Trey Oxford, Steven M. Bierer, Leo Ling, Kaibao Nie, Amy Nowack, Jay T. Rubinstein, and James O. Phillips Electrical Stimulation of the Vestibular Nerve During Head Unrestrained Gaze Shifts. NW Auditory and Vestibular Meeting, Seattle, WA, 2010

James Phillips, Leo Ling, Albert Fuchs, Chris Kaneko, Steven Bierer, Shawn Newlands, Kaibao Nie, Amy Nowack, Trey Oxford, Jay Rubinstein Discharge frequency versus recruitment coding for a unilateral vestibular implant. XXVI Bárány Society Meeting, Reykjavik, Iceland, 2010

James Phillips, Leo Ling, Albert Fuchs, Chris Kaneko, Steven Bierer, Shawn Newlands, Kaibao Nie, Amy Nowack, Trey Oxford, Jay Rubinstein Exploring the mechanism of a vestibular prosthesis. CNCS Retreat, Rochester, NY, 2010

James Phillips, Leo Ling, Albert Fuchs, Chris Kaneko, Steven Bierer, Shawn Newlands, Kaibao Nie, Amy Nowack, Trey Oxford, Jay Rubinstein Tale of a vestibular prosthesis: four years from bench to bedside. NW Auditory and Vestibular Meeting, Seattle, WA, 2010

James Phillips, Leo Ling, Chris Kaneko, Steven Bierer , Kaibao Nie, Jay Rubinstein Bench to bedside: Vestibular and auditory function testing as a translational tool for a vestibular prosthesis. Cajal Club 2010, Seattle, WA

Objectives for Quarter 18.

1. In next quarter, we will complete all device development and turn our activities entirely toward recording behavior and single neuron activity from the monkeys that remain on the protocol.

2. We will begin experiments in two rhesus monkeys using intratympanic gentamicin injection to eliminate hair cell function and treat the loss of function with the implanted vestibular stimulator. We plan to use both tonic unmodulated stimulation and real time modulated stimulation of the lesioned ear to compare the effect of restoring background rate to that of restoring modulated input to the central vestibular system during passive and active natural head rotation.

3. We will continue to perform anatomical reconstruction of the vestibular end organ and brainstem using CT, micro-CT and histological reconstruction of the temporal bone and brain.

4. We will continue to record from single neurons in the abducens nucleus, nucleus prepositus, and the vestibular nuclei to characterize their response during active amplitude modulated electrical stimulation, frequency modulated electrical

stimulation, and combined electrical and rotational stimulation. In addition, we will study the neural basis of the eye position effects described in this report.

5. We will provide final specifications to Dr. Satinderpall Pannu for a first run of deep brain multisite recording electrode arrays. When these devices become available, we will use them in our neural recordings to obtain simultaneous single neuron recordings from additional sites during electrical and rotational stimulation.

6. We will activate the device that was implanted in a human subject to characterize the eye movements and subjective sensation elicited by electrical stimulation of the semicircular canals. We plan to tests several amplitudes and frequencies of stimulation at different durations and compare these results directly to the results obtained in rhesus monkeys.

7. We will present our results in multiple international meetings, submit an additional manuscript for publication, and prepare at least one RO1 application for continued funding of the primate and human vestibular implant research projects.